DIVISION OF MOLECULAR NEUROBIOLOGY

Professor
NODA, Masaharu

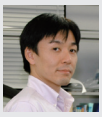

Associate Professor
SHINTANI, Takafumi

Assistant Professor: *SAKUTA, Hiraki*
HIYAMA, Takeshi
Technical Staff: *TAKEUCHI, Yasushi*
NIBB Research Fellow: *MATSUDA, Takashi*
Postdoctoral Fellow: *FUJIKAWA, Akihiro*
SUZUKI, Ryoko
LIN, Chia-Hao
NOMURA, Kengo
SOKENDAI Graduate Student: *TANGA, Naomi*
Visiting Scientist: *YU, Yang*
Technical Assistant: *NAKANISHI, Norie*
WADA, Kotoe
KONISHI, Mie
ISOSHIMA, Yoshiko
Secretary: *KODAMA, Akiko*

The scope of our interests encompasses the underlying mechanisms for the development of the vertebrate central nervous system (CNS) and various functions of the mature brain, including body fluid homeostasis, blood pressure control, food intake control, learning and memory.

I. Mechanisms for learning and memory

Brain-derived neurotrophic factor (BDNF) plays an important role in synaptic plasticity related to learning and memory. While we have previously reported that SPARC-related protein containing immunoglobulin domains 1 (SPIG1, also known as Follistatin-like protein 4, FSTL4) binds to pro-BDNF and negatively regulates BDNF maturation, its neurological functions, particularly in learning and memory, have not yet been elucidated.

To this end, we examined the electrophysiological and behavioral phenotypes of *Spig1*-knockout (*Spig1*-KO) mice. Adult *Spig1*-KO mice exhibited greater excitability and facilitated long-term potentiation (LTP) in the CA1 region of hippocampal slices than age- and sex-matched wild-type (WT) mice (Figure 1A). Facilitated LTP was reduced to the level of WT by the bath application of an anti-BDNF antibody to hippocampal slices. A step-through inhibitory avoidance learning paradigm revealed that the extinction of aversive memories was significantly enhanced in adult *Spig1*-KO mice (Figure 1B), while they showed a normal acquisition of aversive memories. Furthermore, spatial reference memory formation was also normal in the standard Morris water maze task.

An intracerebroventricular (icv) injection of anti-BDNF in the process of extinction learning transiently induced the recurrence of aversive memories in *Spig1*-KO mice, but demonstrated no effects in WT mice. These results indicate a critical role for SPIG1 in BDNF-mediated synaptic plasticity in the extinction of inhibitory avoidance memory.

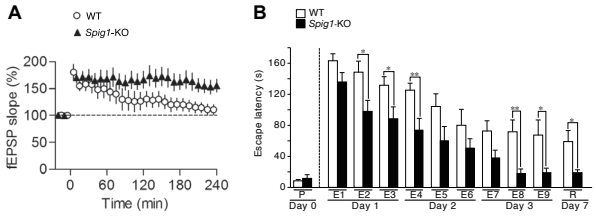

Figure 1. Enhanced LTP in the CA1 region of the hippocampus and enhanced extinction of aversive memories in Spig1-KO mice.
A) Plots of the field excitatory postsynaptic potential (fEPSP) slopes in WT and Spig1-KO mice. n = 9 from 6 mice.
B) Escape latency of WT and Spig1-KO mice. Spig1-KO mice exhibited facilitated extinction of inhibitory avoidance, irrespective of the normal acquisitive of aversive memories.
n = 6 or 7 for each group.

II. Physiological roles of receptor-like protein tyrosine phosphatases

Protein tyrosine phosphorylation plays numerous crucial roles in various biological events such as cellular proliferation, differentiation, survival, migration, and metabolism. Cellular tyrosine phosphorylation levels are governed by the opposing activities of protein tyrosine kinases (PTKs) and protein tyrosine phosphatases (PTPs). However, the physiological functions and regulatory mechanisms of receptor-like PTPs (RPTPs) have not been fully elucidated. We have been making efforts to reveal the functional roles of RPTPs, especially of the R3 and R5 subfamilies.

2-1. R3 RPTP subfamily

Eph receptors play a pivotal role in the axon guidance of retinal ganglion cells (RGCs) at the optic chiasm and the establishment of the topographic retinocollicular map. We previously demonstrated that protein tyrosine phosphatase receptor type O (PTPRO) is specifically involved in the control of retinotectal projections in chicks through the dephosphorylation of EphA and EphB receptors. We subsequently revealed that all the mouse R3 subfamily members (PTPRB, PTPRH, PTPRJ, and PTPRO) of the RPTP family inhibited Eph receptors as their substrates in cultured mammalian cells.

We investigated the functional roles of R3 RPTPs in the retinocollicular projection in mice. *Ptpro* and *Ptprj* were expressed in mouse RGCs; however, *Ptprj* expression levels were markedly higher than those of *Ptpro*. Consistent with their expression levels, Eph receptor activity was significantly enhanced in *Ptprj*-knockout (*Ptprj*-KO) retinas. In *Ptprj*-KO and *Ptprj*/*Ptpro*-double-KO (DKO) mice, the number of retinal axons that projected ipsilaterally or to the contralateral eye was significantly increased (Figure 2). Furthermore, retinal axons in *Ptprj*-KO and DKO mice formed anteriorly shifted ectopic terminal zones in the superior colliculus (SC).

We found that c-Abl (Abelson tyrosine kinase) was downstream of ephrin-Eph signaling for the repulsion of retinal axons at the optic chiasm (OC) and in the SC. c-Abl was identified as a novel substrate for PTPRJ and PTPRO, and the phosphorylation of c-Abl was upregulated in *Ptprj*-KO and DKO retinas. Thus, PTPRJ regulates retinocollicular projections in mice by controlling the activity of Eph and c-Abl kinases.

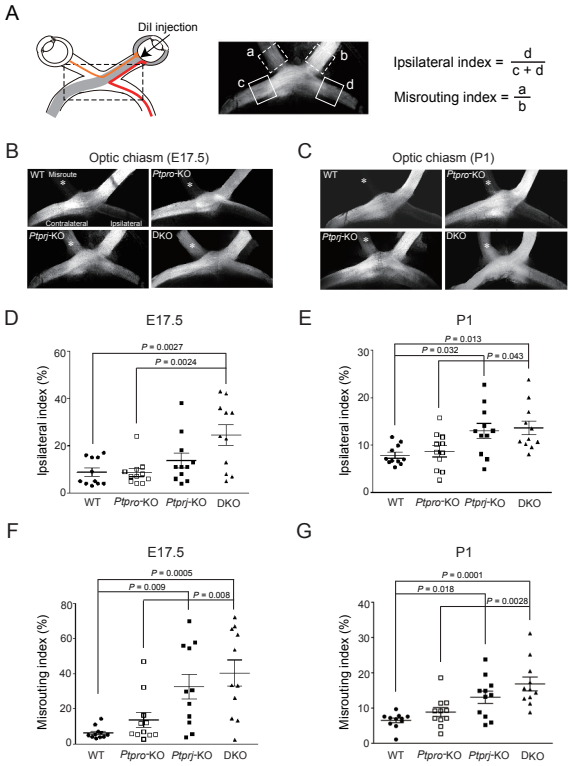

Figure 2. Ipsilateral projections of retinal axons at the OC in WT, *Ptpro*-KO, *Ptprj*-KO, and DKO mice.

A) Schematic representation of DiI tracing of retinal axons and quantification of the projection index to the ipsilateral side or contralateral eye. Retinal axons in the right eye were anterogradely labeled with DiI. Axons that projected ipsilaterally and misrouted to the contralateral eyes are indicated by red and orange lines, respectively. The ipsilateral index was calculated by dividing the fluorescent intensity of the ipsilateral optic tract by the total fluorescent intensity of both tracts. The misrouting index was calculated as the ratio between the fluorescent intensity of the left optic nerve and that of the right optic nerve.

B & C) Representative whole-mount ventral view of retinal axons at the OCs in WT, *Ptpro*-KO, *Ptprj*-KO, and DKO mice. Retinal axons in the right eye were labeled with DiI at E17.5 (B) and P1 (C). Arrows and asterisks indicate projections to the iplilateral side and contralateral optic nerve, respectively. Scale bars, 200 μm.

D & E) Index of projections to the ipsilateral side. n = 11 for each group.

F & G) Index of projections to the contralateral optic nerve. n = 11 for each group.

2-2. R5 RPTP subfamily

PTPRZ is one of the most abundant PTPs in oligodendrocyte precursor cells (OPCs), which are the principal source of myelinating oligodendrocytes. Three PTPRZ isoforms are generated by alternative splicing from a single gene: two transmembrane isoforms, PTPRZ-A and PTPRZ-B, and one secretory isoform, PTPRZ-S (or phosphacan). All isoforms are heavily modified with chondroitin sulfate (CS) chains, and identified as chondroitin sulfate proteoglycans (CSPGs) in the CNS. The CS moiety on the extracellular domain of PTPRZ is essential for achieving high-affinity binding sites for the endogenous ligands, such as pleiotrophin (PTN). We previously postulated that PTPRZ is a new molecular target in the development of drugs that treat glioblastoma and demyelinating diseases, such as multiple sclerosis (MS).

We have already revealed that PTPRZ functions to maintain OPCs in an undifferentiated state. We are now investigating (1) the overall picture of downstream signaling pathways involved in OPC differentiation, (2) the molecular basis of the PTN-induced inactivation of PTPRZ receptors, and (3) whether PTPRZ isoforms play a distinct physiological role by characterizing neurological phenotypes of two different knock-in mutant mouse strains carrying targeted loss of receptor functions of PTPRZ in comparison with *Ptprz*-null mice. Regarding (1), we recently reported that the PTN-PTPRZ signal activated the AFAP1L2-dependent PI3K-AKT pathway for oligodendrocyte differentiation (Tanga, N., *et al.*, Glia. doi: 10.1002/glia.23583).

III. Brain systems for body-fluid homeostasis

We have shown that Na_x, which structurally resembles voltage-gated sodium channels ($Na_v1.1$–1.9), is the brain $[Na^+]$ sensor to detect increases in $[Na^+]$ in body fluids. Na_x is preferentially expressed in specific glial cells of sensory circumventricular organs (sCVOs) including the subfornical organ (SFO) and organum vasculosum lamina terminalis (OVLT). These regions are known as brain loci that are substantially lacking a blood-brain barrier. We have already reported that Na_x signals in these brain regions are involved in the control of water and salt intake.

3-1. Central mechanisms of salt-induced hypertension through activation of sympathetic nerve activities

Hypertension is a major risk factor for cardiovascular disease worldwide, and approximately 40% (1 billion) of adults aged 25 and above have been diagnosed with hypertension (World Health Organization 2013). A positive correlation between salt (NaCl) intake and blood pressure (BP) has long been postulated. A battery of studies has shown that a diet high in salt increases sodium concentrations ($[Na^+]$) in plasma and the cerebrospinal fluid (CSF). $[Na^+]$ elevations in plasma and CSF enhance sympathetic nerve activity (SNA), leading to increases in BP. However, underlying mechanisms responsible for $[Na^+]$ sensing and signaling pathways to induce sympathetically-mediated BP elevations have not yet been elucidated.

We have recently revealed that sympathetic activation leading to BP increases was not induced in *Na_x*-KO mice by mandatory high salt (HS) intakes or the intraperitoneal/

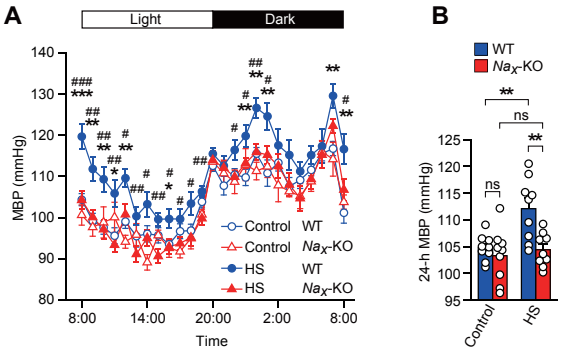

Figure 3. High salt (HS) ingestion induces an increase in $[Na^+]$ in body fluids that drives sympathetically mediated BP elevations in WT, but not in *Na_x*-KO mice.

A) Circadian changes in mean blood pressure (MBP) in control and HS-ingested mice. n = 9 mice for each. $^{*}p < 0.05$, $^{**}p < 0.01$, $^{***}p < 0.001$ (control WT versus HS-ingested WT); $^{\#}p < 0.05$, $^{\#\#}p < 0.01$, $^{\#\#\#}p < 0.001$ (HS-ingested WT versus HS-ingested *Na_x*-KO).

B) Average MBP over a 24-hr period in control and HS-ingested mice. n = 9 for each.

intracerebroventricular infusions of hypertonic NaCl solutions, in contrast to WT mice (Figures 3 and 4). In the present study, we identified that Na_x channels in the OVLT play the role of a sensor detecting increases in [Na^+] in body fluids for BP control. In the OVLT, elevations in extracellular [Na^+] activated Na_x, and the Na^+ influx consequently leads to stimulation of anaerobic glycolysis in Na_x-positive glial cells to generate lactate. H^+ and lactate were then released from the glial cells through H^+/lactate symporters (monocarboxylate transporter, MCT). The released H^+ stimulated OVLT neurons projecting to the paraventricular hypothalamic nucleus (PVN) [OVLT(→PVN) neurons]. The H^+-dependent activation of OVLT(→PVN) neurons was mediated by acid-sensing ion channel 1a (ASIC1a) in the neurons. OVLT(→PVN) neurons activate PVN neurons and then rostral ventrolateral medulla (RVLM) neurons to increase SNA leading to BP elevations (Figure 5).

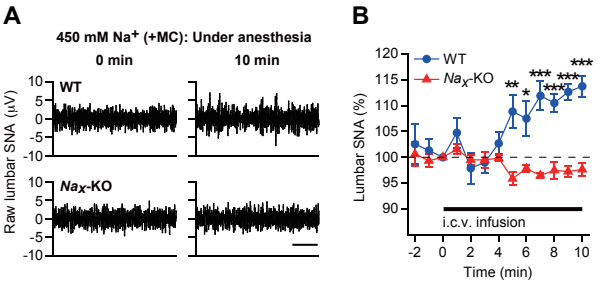

Figure 4. Lumbar SNA is stimulated by i.c.v. infusion of hypertonic Na solution in WT mice, but not in Na_x-KO mice.
A) A representative raw record of lumbar SNA just before (0 min) and 10 min after the i.c.v. infusion of hypertonic Na solution. Scale bar, 0.1 s. MC, Manning compound (a blocker of vasopressin receptor 1a).
B) Changes in lumbar SNA in response to the i.c.v. infusion of hypertonic Na solution. $n = 6$ each. The value at 0 min was set to 100%.

These molecular and cellular processes are the first steps in the activiation of the neurogenic mechanisms responsible for BP elevations in response to [Na^+] increases in the blood and CSF. Our results may provide novel neural therapeutic targets and encourage the future potential for treating a salt-sensitive phenotype in humans.

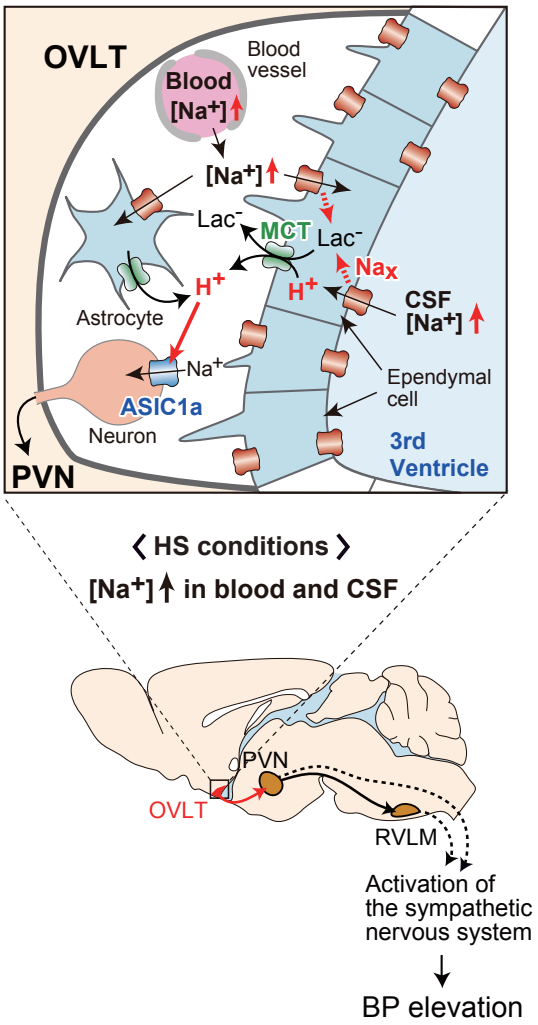

Figure 5. Central mechanisms of salt-induced BP elevations.
Upper: Increases in blood and CSF [Na^+] activate Na_x in the OVLT, and induce lactate (Lac^-) and H^+ release from Na_x-expressing ependymal cells through MCT. The resultant extracellular acidification (H^+) stimulates OVLT(→PVN) neurons via ASIC1a activation.
Lower: The OVLT-PVN-RVLM neural pathway is then activated and elevates BP through increases in SNA.

Publication List:

〔Original papers〕

- Suzuki, R., Fujikawa, A., Komatsu, Y., Kuboyama, K., Tanga, N., and Noda, M. (2018). Enhanced extinction of aversive memories in mice lacking SPARC-related protein containing immunoglobulin domains 1 (SPIG1/FSTL4). Neurobiol. Learn. Mem. *152*, 61-70.
- Yang, Y., Shintani, T., Takeuchi, Y., Shirasawa, T., and Noda, M. (2018). Protein tyrosine phosphatase receptor type J (PTPRJ) regulates retinal axonal projections by inhibiting Eph and Ab1 kinases in mice. J. Neurosci. *38*, 8345-8363.

〔Original paper (E-publication ahead of print)〕

- Nomura, K., Hiyama, T.Y., Sakuta, H., Matsuda, T., Lin, C.-H., Kobayashi, K., Kobayashi, K., Kuwaki, T., Takahashi, K., Matsui, S., and Noda, M. [Na^+] increases in body fluids sensed by central Na_x induce sympathetically mediated blood pressure elevations via H^+-dependent activation of ASIC1a. Neuron 2018 Nov 29.